3D Time Domain Boundary Element Formulation for Anisotropic Elastic Solid

Alan T. Tan [1], Sohichi Hirose [2]

1) Center for Urban Earthquake Engineering, Tokyo Institute of Technology (2-21-1, O-okayama, Meguro-ku, Tokyo 152-8552, E-mail: tan.a.aa@m.titech.ac.jp)

2) Department of Mechanical and Environmental Informatics, Tokyo Institute of Technology (2-21-1, O-okayama, Meguro-ku, Tokyo 152-8552, E-mail: shirose@cv.titech.ac.jp)

The formulation of the time domain boundary element method for 3D anisotropic elastic solids is presented here. The fundamental solutions used are the ones developed by Wang and Achenbach [1] and are separated into static parts and dynamic parts. Radon transform and inverse Radon transform were used to derive the fundamental solutions. Thus, the solutions contain integrals over a unit sphere. For the static parts, these integrals are dealt with analytically with the help of integration by residues. However, the integrals in the dynamic parts can only be integrated numerically. Boundary integral equations also require the presence of spatial integrals and the proposed approach is to compute spatial integrals using Gaussian quadrature for triangular elements. But these integrals should be dealt with proper care because of the inherent singularities and other possible numerical problems. To check the validity of the codes, the fundamental solutions are compared to isotropic solutions. Additionally for the time convolution, approximating functions are needed to be chosen properly.

Key words: anisotropic, boundary element method, dynamic, three dimensional

1. Introduction

This document contains the details of the formulation of the time domain boundary element method for three dimensional anisotropic elastic solids. Furthermore, the method of tackling the numerically computations are added. Fundamentals solutions and the corresponding stress fields are very important in the implementation of the boundary element method (BEM). Wang and Achenbach [1] derived the fundamental solutions for generally anisotropic elastic solids and these are much more complex compared to their isotropic counterparts. In this paper, the numerical computation of the fundamental solutions is shown and these are validated with existing solutions. Then explicit integration schemes for the BEM code are developed.

2. Problem statement

Consider a three dimensional homogeneous and linearly anisotropic solid. The solid is modeled assuming an infinite solid with a cavity of arbitrary shape. Fig. 1 shows the model with an incident wave acting upon the solid. The equations of motion and the constitutive equations are written as follows,

$$\sigma_{ji,j} + f_i = \rho \ddot{u}_i \tag{1}$$

$$\sigma_{ij} = c_{ijkl} u_{k,l} \tag{2}$$

where u_i are the displacements, σ_{ji} is the stress components, c_{ijkl} are the material properties, ρ is the material density and f_i are the body forces. Throughout this paper, a comma after a quantity denotes partial derivative with respect to the spatial variables while a dot appearing on the top of a quantity denotes partial derivative with respect to time. The summation convention rule over repeated indices is used. Lower case roman suffixes take values of 1, 2, and 3.
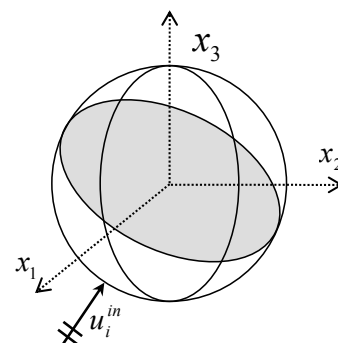

Fig. 1 Model of cavity or inclusion in anisotropic elastic solid

Substituting eq.(2) into eq. (1) and assuming no body forces, the equations of motion are now in terms of the displacement components

$$\left\{\Gamma_{ij}(\partial) - \rho\delta_{ij}\partial_t^2\right\}u_j(\mathbf{x},t) = 0 \tag{3}$$

where

$$\Gamma_{ij}(\partial) = c_{ijkl}\partial_k\partial_l \tag{4}$$

are the terms of the Cristoffel tensor and ∂_k represent partial derivative with respect to x_k. Zero initial conditions are assumed.

3. Boundary integral equations

The boundary integral equations for the displacement components can be written as:

$$u_k^{in}(\mathbf{y},t) + \int_S g_{ik}[\mathbf{x}-\mathbf{y},t] * t_i(\mathbf{x},t)ds_x$$

$$-\int_S h_{ik}[(\mathbf{x}-\mathbf{y}),\mathbf{e}(\mathbf{x}),t] * u_i(\mathbf{x},t)ds_x = \begin{cases} u_k(\mathbf{y},t) & \mathbf{y}\in D \\ \Omega_{ik}(\mathbf{y})u_i(\mathbf{y},t) & \mathbf{y}\in S \\ 0 & \text{otherwise} \end{cases} \tag{5}$$

where $\mathbf{x}$ and $\mathbf{y}$ are the source and the observation points, g_{ik} are the displacement fundamental solutions and h_{ik} are the traction fundamental solutions, u_i are the displacements and t_i are the tractions, Ω_{ik} is the free term, S is the boundary of a scatterer and "in" denotes incident wave. $*$ denotes the time convolution. D denotes the domain.

4. Fundamental solutions

The boundary integral equations of eq.(5) require the fundamental solutions. If we consider a homogeneous anisotropic and linearly elastic solid in a 3D unbounded domain with fixed rectangular coordinate system, the fundamental solutions are described as the solutions of the following differential equations,

$$\left\{c_{ijpq}\partial_j\partial_q - \rho\delta_{ip}\partial_t^2\right\}g_{pk}(\mathbf{x},t) = -\delta_{ik}\delta(\mathbf{x})\delta(t) \tag{6}$$

and with initial conditions,

$$g_{pk}(\mathbf{x},t) = 0 \text{ for } t < 0 \tag{7}$$

where δ_{ik} are the components of the Kronecker delta, $\delta()$ is the delta function and ρ is the material density. Wang and Achenbach [1], using Radon transform, were able to derive expressions for the fundamental solutions in terms of integration over a unit sphere. The displacement fundamental solutions are given as

$$g_{pk}(\mathbf{x},t) = \frac{-H(t)}{8\pi^2}\int_{|n|=1}\sum_{l=1}^{3}\frac{P_{pk}^l}{\rho c_l^2}\partial_t\delta(c_l t - \mathbf{n}\cdot\mathbf{x})d\mathbf{n} \tag{8}$$

where the projectors, given in terms of the adjoints of

$A_{pk}^l = adj\left\{c_{pmkq}n_m n_q - \rho c_l^2\delta_{pk}\right\}$, are $\quad P_{pk}^l = A_{pk}^l / A_{mm}^l$, c_l are

the velocities of the material and $\mathbf{n}$ is a unit vector. Consider the time convolution of g_{pk} and of any function f(t), using some manipulations (integration by parts and transfer of derivatives), the fundamental solutions can be separated into static (S) and dynamic (R) parts as

$$g_{pk}(\mathbf{x},t) * f(t) = g_{pk}^S(\mathbf{x})f(t) + g_{pk}^R\left[\mathbf{x};\dot{f}(t)\right] \tag{9}$$

$$g_{pk}^S(\mathbf{x}) = \frac{1}{8\pi^2}\int_{|n|=1}\Gamma_{pk}^{-1}(\mathbf{n})\delta(\mathbf{n}\cdot(\mathbf{x}-\mathbf{y}))d\mathbf{n} \tag{10}$$

$$g_{ij}^R\left[\mathbf{x};\dot{f}(t)\right] = \frac{-1}{8\pi^2}\int_{\substack{|n|=1\\n\cdot x>0}}\sum_{l=1}^{3}\frac{P_{ij}^l}{\rho c_l^3}\dot{f}\left(t - c_l^{-1}(\mathbf{n}\cdot x)\right)d\mathbf{n} \tag{11}$$

The fundamental solutions include integrations over a unit sphere (due to the inverse Radon transform).
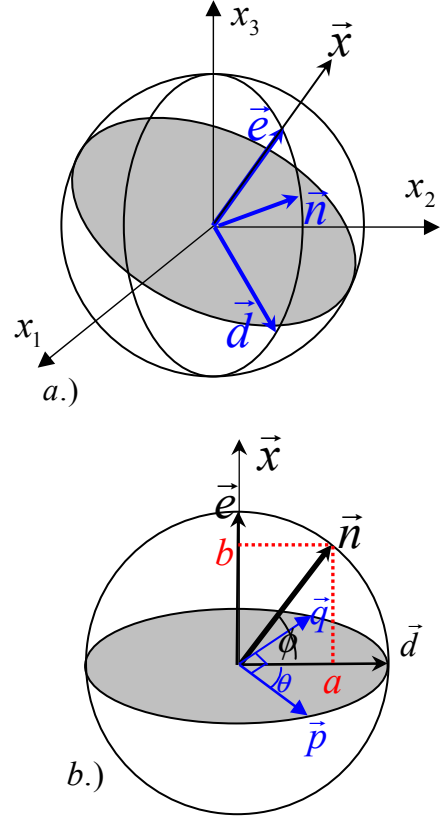

Fig. 2 a.) Geometry of $\mathbf{x}$, $\mathbf{e}$, $\mathbf{d}$ and $\mathbf{n}$ in the fixed coordinates. b.) Geometry n in terms of $\mathbf{p}$ and $\mathbf{q}$

The static singular parts of the displacement fundamental solutions are transformed into explicit expressions by using the residue theorem. The analytical integration by residues is done by first introducing the coordinates shown in Fig. 2a and using these coordinates eq. (10) can be transformed and integrated as

$$g_{pk}^S(\mathbf{x}) = \frac{-\text{Im}}{2\pi r}\sum_{l=1}^{3}\left[\frac{A_{pk}^l(\mathbf{p}+\zeta\mathbf{q})}{\partial_\zeta D(\mathbf{p}+\zeta\mathbf{q})}\right]_{\zeta=\zeta_l} \tag{12}$$

where r=|$\mathbf{x}$|, Im means imaginary parts, $\mathbf{q}$ and $\mathbf{p}$ are orthonormal vectors in the plane normal to $\mathbf{e}$ shown in Fig. 2b. , and D($\mathbf{n}$) is the determinant of $\left[c_{pmkq}n_m n_q - \rho c_l^2\delta_{pk}\right]$ and ζ_l are the roots of the determinant equation. The integration for the dynamic parts cannot be calculated analytically. Again using coordinates of Fig. 2, eq. (11) can be rewritten as

$$g_{pk}^{R}\left[\boldsymbol{x};\dot{f}(t)\right]$$
$$=\frac{-1}{8\pi^{2}}\int_{0}^{\pi/2}\int_{0}^{2\pi}\sum_{l=1}^{3}\frac{P_{pk}^{l}}{\rho c_{l}^{3}}\dot{f}\left(t-c_{l}^{-1}r\sin\theta\right)\left|\cos\theta\right|d\phi d\theta \tag{13}$$

where Gaussian quadrature is used to calculate the integral over the unit sphere. Analytical integration is not possible here because projectors P_{lpk} and velocities c_l are dependent on $\boldsymbol{n}$ and thus on θ and ϕ. The presence of the absolute value of cosine is due to the integration over the surface of a unit sphere.

Again reconsidering the boundary integral equations of eq. (5), traction fundamental terms are also needed. The traction fundamental solutions can be calculated by substituting eq. (8) into Hooke's law.

$$h_{ij}(\boldsymbol{x},\boldsymbol{e},t)=c_{impn}e_{m}\left(\boldsymbol{x}\right)\frac{\partial}{\partial x_{n}}g_{pj}\left(\boldsymbol{x},t\right) \tag{14}$$

where e_m are the components of the unit normal vector. The convolution of $\boldsymbol{h}$ and f, after some manipulations, can be written as

$$h_{ij}(\boldsymbol{x},\boldsymbol{e},t)*f(t)=\frac{1}{8\pi^{2}}\int_{|n|=1}\sum_{l=1}^{L}Q_{ij}^{l}\left\{\begin{bmatrix}\frac{\partial}{\partial\tau}\left[\delta(c_{l}\tau-\boldsymbol{n}\cdot\boldsymbol{x})\right]f(t-\tau)\end{bmatrix}_{0}^{t}\\+\frac{1}{c_{l}}\ddot{f}\left(t-c_{l}^{-1}(\boldsymbol{n}\cdot\boldsymbol{x})\right)\end{pmatrix}d\boldsymbol{n} \tag{15}$$
$$=h_{ij}^{S}(\boldsymbol{x})f(t)+h_{ij}^{R}\left[\boldsymbol{x};\ddot{f}(t)\right]$$

$$h_{ij}^{S}\left(\boldsymbol{x}\right)=\frac{1}{8\pi^{2}}\int_{|n|=1}\sum_{l=1}^{L}Q_{ij}^{l}\dot{\delta}\left(\boldsymbol{n}\cdot\boldsymbol{x}\right)d\boldsymbol{n} \tag{16}$$

$$h_{ij}^{R}\left[\boldsymbol{x};\ddot{f}(t)\right]=\frac{1}{8\pi^{2}}\int_{\substack{|n|=1\\\boldsymbol{n}\cdot\boldsymbol{x}>0}}\sum_{l=1}^{L}Q_{ij}^{l}\ddot{f}\left(t-c_{l}^{-1}(\boldsymbol{n}\cdot\boldsymbol{x})\right)d\boldsymbol{n} \tag{17}$$

where $Q_{ij}^{l}=c_{impn}e_{m}\left(\boldsymbol{x}\right)\dfrac{n_{n}P_{pj}^{l}\left(\boldsymbol{n}\right)}{\rho c_{l}^{4}}$

Although eq. (16) is equivalent to the traction static parts, it will is not very useful for the boundary element formulation because it is not very easy to deal with derivatives of the delta function. Recall that the explicit forms of the displacement fundamental solutions are available in eq. (12). Taking advantage of this and substituting into Hooke's Law, the static traction parts can be rewritten but again explicit expressions of these are quite complicated. However, developing a method where the integral kernel for $\boldsymbol{h}$ in eq. (5) is taken into account looks promising. The convolution of $g_{pk,i}$ and any function f along a curve l [2,3] can be used to simplify the kernel. Fig. 3 shows the diagram for the curve l, the field and source points, and the unit vectors needed for the calculation. Using Wang's method [2], $g^{S}_{ik,q}$ can be written as:

$$g_{jk,q}^{S}\left(x(l)-y\right)=\frac{\partial}{\partial l}V_{jkq}\left(y,l\right)+W_{jkq}\left(y,l\right)$$
$$V_{jkq}\left(y,l\right)=\frac{1}{8\pi^{2}}\int_{|n|=1}\frac{n_{q}A_{jk}\left(n\right)}{D\left(n\right)\left(n\cdot v\right)}\delta\left(n\cdot\bar{x}\right)dn \tag{18}$$
$$W_{jkq}\left(y,l\right)=\frac{\kappa}{8\pi^{2}}\int_{|n|=1}\frac{\left(n\cdot w\right)n_{q}A_{jk}\left(n\right)}{\left(n\cdot v\right)^{2}D\left(n\right)}\delta\left(n\cdot\bar{x}\right)dn$$

where $\bar{x}=x(l)-y$, $v=\dfrac{\partial x}{\partial l}$, $\omega=\dfrac{\partial^{2}x}{\partial l^{2}}\Big/\kappa$, $\kappa=\left|\omega\right|$.
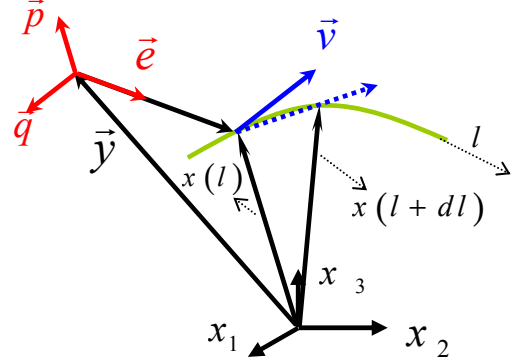
Fig. 3. Geometry of $(\boldsymbol{p},\boldsymbol{q},\boldsymbol{e})$ along curve l

Following the steps for the displacement fundamental solutions, analytical solutions for $\boldsymbol{V}$ and $\boldsymbol{W}$ can be analytically calculated as

$$V_{ipq}\left(y,l\right)=\frac{-\text{Im}}{2\pi h}\sum_{l=1}^{3}\left[\frac{\left(p_{q}+\zeta q_{q}\right)A_{ip}\left(\vec{p}+\zeta\vec{q}\right)}{\zeta\partial_{\zeta}D\left(\vec{p}+\zeta\vec{q}\right)}\right]_{\zeta=\zeta_{l}}$$
$$W_{ipq}\left(y,l\right)=\frac{-\text{Im}\kappa}{2\pi h^{2}}\sum_{l=1}^{3}\left[\frac{\left(\alpha+\beta\zeta\right)\left(p_{q}+\zeta q_{q}\right)A_{ip}\left(\vec{p}+\zeta\vec{q}\right)}{\zeta^{2}\partial_{\zeta}D\left(\vec{p}+\zeta\vec{q}\right)}\right]_{\zeta=\zeta_{l}} \tag{19}$$

where $\alpha=(\text{p}\cdot\text{w})r$, $\beta=(\text{q}\cdot\text{w})r$, $h=(\text{q}\cdot\text{v})r$. If a linear curve l is used, the function can be further simplified to

$$g_{jk,q}^{S}\left(x(l)-y\right)=\frac{\partial}{\partial l}V_{jkq}\left(y,l\right), \tag{20}$$

and with the given form, the integral along a line element can be easily (analytically) computed.

For the dynamic traction parts, eq. (17) is used and can be calculated numerically using Gaussian quadrature and written

$$h_{ij}^{R}\left[\boldsymbol{x},\ddot{f}(t)\right]=\frac{1}{8\pi^{2}}\int_{0}^{\pi/2}\int_{0}^{2\pi}\sum_{l=1}^{3}Q_{ij}^{l}\ddot{f}\left(t-c_{l}^{-1}r\sin\theta\right)\left|\cos\theta\right|d\phi d\theta \tag{21}$$

5. Implementation of the formulation

In solving the boundary integral equation, the separated values of the fundamental solutions are used and can be rewritten in the following form:

$$\Omega_{ik}(\boldsymbol{y})u_{i}(\boldsymbol{y},t)=u_{k}^{in}(\boldsymbol{y},t)+\int_{S}g_{ik}^{S}(\boldsymbol{x}-\boldsymbol{y})t_{i}(\boldsymbol{x},t)ds_{\boldsymbol{x}}$$
$$+\int_{S}g_{pk}^{R}\left[(\boldsymbol{x}-\boldsymbol{y});\dot{t}_{i}(\boldsymbol{x},t)\right]ds_{\boldsymbol{x}}$$
$$-\int_{S}h_{ik}^{S}\left[(\boldsymbol{x}-\boldsymbol{y}),e(\boldsymbol{x});t\right]u_{i}(\boldsymbol{x},t)ds_{\boldsymbol{x}}$$
$$-\int_{S}h_{ik}^{R}\left[(\boldsymbol{x}-\boldsymbol{y});\ddot{u}_{i}(\boldsymbol{x},t)\right]ds_{\boldsymbol{x}} \tag{22}$$

The time stepping method is a process used to approximate the values at a finite number of times intervals. Thus, the boundary integral equation can then be approximated by linear algebraic system of equations which can be solved using numerical method. The proper selection of the shape functions could make the problem easier to deal with.
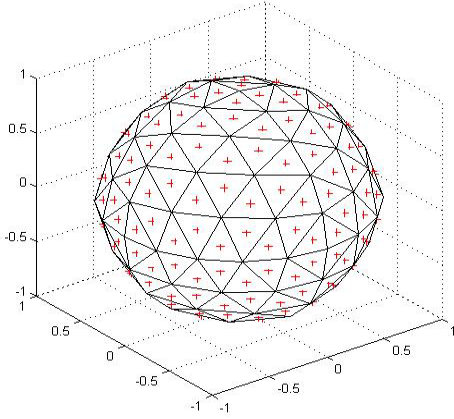
Fig. 4 Sample of sphere discretized using triangular elements with the crosses as the midpoint of the triangle

Triangular elements are chosen to discretize the surface or boundary. Fig. 4 shows a sample spherical cavity and is discretized using triangular elements.

The variables or fields in the boundary are approximated as

$$u_i(x,t) \approx \sum_{n=1}^{N}\sum_{k=1}^{K} \phi_u^n(x)\varphi_u^k(t)u_i^{nk}$$
$$t_i(x,t) \approx \sum_{n=1}^{N}\sum_{k=1}^{K} \phi_t^n(x)\varphi_t^k(t)t_i^{nk}$$
$$(23)$$

where $\phi_u^n(x)$, $\phi_t^n(x)$ are the spatial shape functions and are constants per element and $\varphi_u^k(x)$, $\varphi_t^k(x)$ are the temporal shape functions. n denotes the element number while the capital N denotes the total number of elements. This is the same for k and K, denoting kth time and total time steps. The temporal shape functions are chosen carefully. Higher order temporal shape functions are used and the second derivative of the displacement temporal function as well as the first derivative of the traction temporal shape function should result to the Heaviside functions. This is needed to be done to make the kernels G^R and H^R simple. Therefore, quadratic displacement temporal shape functions are needed while linear traction temporal shape functions are required.

Substitution of eq. (23) into eq. (22.b) leads to a system of linear equations

$$\Omega_{IK}^m U_I^{mQ} = U_K^{in,mQ} + \sum_{n=1}^{N} G_{IK}^{S;mn} T_I^{nQ} + \sum_{n=1}^{N}\left(\sum_{q=1}^{Q} G_{IK}^{R;m,n,q}\right)T_I^{nq}$$
$$-\sum_{n=1}^{N} H_{IK}^{S;mn} U_I^{nQ} - \sum_{n=1}^{N}\left(\sum_{q=1}^{Q} H_{IK}^{R;m,n,q}\right)U_I^{nq}$$
$$(24)$$

where **G** and **H** are the kernels of the displacement fundamental solutions and the traction fundamental solutions, respectively.

The boundary integral equations require the presence of spatial integrals. Special care is needed to properly compute the spatial integrals because of the presence of singularities inherent in the static parts and other possible numerical problems. The singularities occur if the source point is in the boundary element.

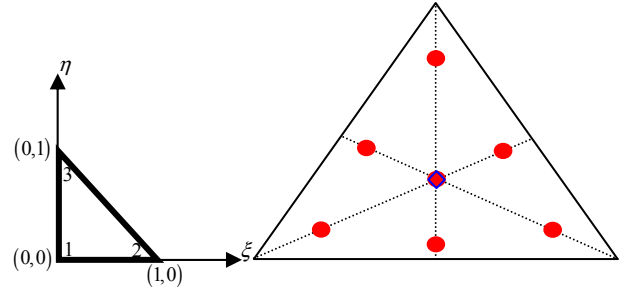To solve the kernels of eq. (24), different methods are to used.

Fig. 5 Master element and the Gaussian quadrature points in a sample triangle.

Displacement static parts nonsingular. For usual nonsingular spatial integrals or nonsingular G^S, Gaussian quadrature for triangular elements is used except for the traction static parts. Fig. 5 shows the Gaussian quadrature points in a sample triangle.

Displacement static parts singular. For the singular integrals in G^S, it can be noted in that for **y** inside the element, the fundamental solutions become a function of r. The term below is constant in terms of θ.

$$\frac{\text{Im}}{2\pi}\sum_{m=1}^{3}\left[\frac{A_{ij}(\vec{p}+\zeta\vec{q})}{\partial_\zeta D(\vec{p}+\zeta\vec{q})}\right]_{\zeta=\zeta_m} \to \text{constant in } \theta \qquad (25)$$

Therefore the integrals are rewritten in polar coordinates and integrated analytically along the radius and numerically in terms of the angle as shown here.

$$\int_{\theta_1}^{\theta_2}\int_{0}^{r(\theta)}\left[\frac{f(\theta)}{r}r\,dr\right]d\theta = \int_{\theta_1}^{\theta_2} f(\theta)r(\theta)d\theta \qquad (26)$$

The triangle is first divided into three parts as shown in Fig. 6. Then each part is to be integrated analytically. The angles can be determined from the master element and subsequently used to all singular triangles.
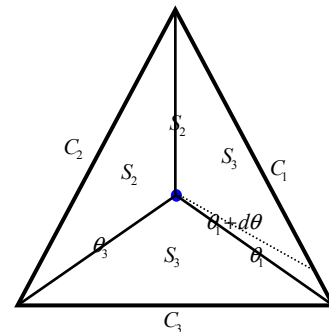

Fig. 6 Division of the sample triangle for integration of singular parts.

Traction static parts. For the traction static parts, the spatial integrals are rewritten in terms of line integrals and thus can be integrated analytically if the line or path is properly chosen [3]. Figure 7 shows the integration points and Simpson's method is

used for the integration. Other methods can be used to replace Simpson's method and should still remain at the edges of triangle but the position can be change depending on the method used (i.e. Gaussian quadrature in 1-D).
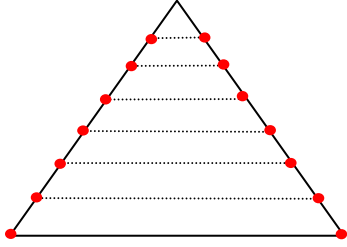

Fig. 7 Integration points for the traction static parts..

For all other kernels (ie, G^R and H^R), Gaussian quadrature is used for the spatial integration. It should be noted that time convolutions are not needed here because it was reduced to derivatives with respect to time in eqns. (9) and (15). Thus, the calculation of the kernels became more difficult (as compared to its 2D counterpart where delta function was used extensively). The presence of $\ddot{u}\left(t - c_l^{-1}\left(\mathbf{n} \cdot \mathbf{x}\right)\right)$ and $\dot{i}\left(t - c_l^{-1}\left(\mathbf{n} \cdot \mathbf{x}\right)\right)$ in the kernels complicates things. But with quadratic ψ_u and linear ψ_t, these derivatives are constant and makes it easier to solve the kernels.

6. Numerical results

The static parts are compared to the isotropic formulation by using an isotropic solid having wave-speed quotient of $c_L/c_T = 2$. Table 1 gives the normalized static fundamental displacements as calculated for the given field point and the source point is at the origin. The values for the displacements are compared and show good agreement for the given quantities.
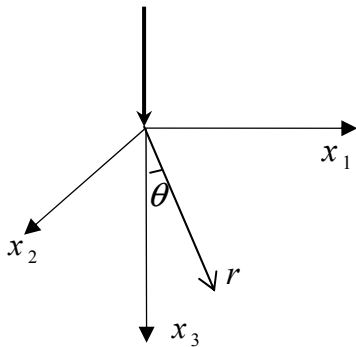

Fig. 8. Geometry of the point load in an unbounded solid.

To validate the dynamic parts, time displacement $g_{33}(x,t)$ are calculated using eq.(9). These are computed for a time dependence of a point load shown in Fig. 8 with equation given as

$$f\left(\tau\right) = \tau^2 e^{-3\tau^2} H\left(\tau\right) \quad \text{with} \quad \tau = \left(c_{44}/\rho\right)^{1/2} t/a \qquad (27)$$

where a=1, and solutions are evaluated at τ =5.0 and are plotted along radial lines as shown in Fig. 9 . Numerical solutions for an isotropic solid and ice are also shown. Ice is a transversely isotropic solid and the axis of symmetry is taken as x_3. The

nonzero constants are $c_{11}=c_{22}$, c_{33}, $c_{13}=c_{23}$, c_{12}, $c_{44}=c_{55}$, $c_{66}=1/2(c_{11}-c_{12})$. For ice, $c_{11}=1.38$, $c_{33}=1.50$, $c_{12}=0.71$, $c_{13}=0.58$, $c_{44}=0.32$.

Table 1. Normalized static fundamental displacements calculated with isotropic formulation and present formulation

(x,y,z)	Isotropic formulation g_{33}	Present formulation g_{33}
(0.001, 0.0, 0.0)	6.6290395	6.6267620
(0.01, 2.25, 0.63)	0.0029407	0.0029392
(0.02, 4.75, 1.33)	0.0013930	0.0013923
(0.022, 5.25,1.47)	0.0012603	0.0012597
(0.035, 8.5, 2.38)	0.0007784	0.0007780
(0.05, 12.25, 3.43)	0.0005401	0.0005399

In Fig. 9 where $\theta=0$, computed values for an isotropic solid are compared to Wang's paper [1] and in turn where compared to analytical solutions. Different values of θ are plotted along radial lines from the point of application of the load which is at the origin. Figs. 10 show the values of the ones for ice.
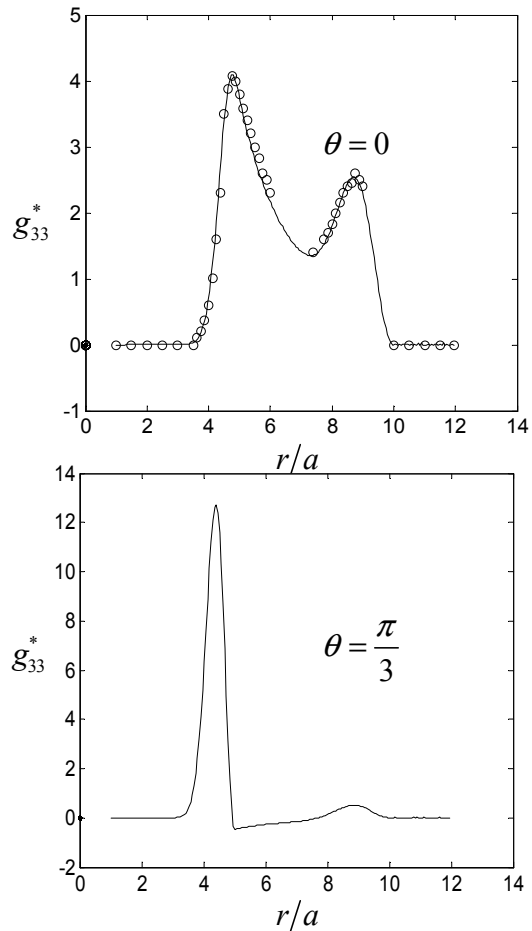

Fig. 9. Dimensionless displacement in an isotropic

solid: $g_{33}^* = \left(800\pi^2 a c_{44}\right) g_{33}\left(x,t\right)$ versus r/a.

7. Summary

Numerical calculation of the explicit 3D time domain fundamental solutions are presented here and the algorithms are given in a way easily incorporated into the boundary element code. The singular parts for displacements are evaluated analytically. Similarly the singular parts for the traction are also evaluated analytically but it is calculated as a line integral over a chosen curve. This plays well into the BEM because the method is integrated over a surface (for 3D) and thus line integrals can be incorporated here. The dynamic parts for both the displacements and tractions are to be calculated using numerical methods. One concern for the dynamic parts is the determination of projectors and the velocities. Possible solution is the use of cubic spline for three inputs. Further application of this numerical method will be investigated. The formulation of the boundary element method is also presented here with the triangular constant elements chosen to make the calculation simpler. Proposed numerical calculations are also shown and analyzed. Currently, the development of the BEM code is being written.

References

[1] C.Y. Wang and J.D. Achenbach, Elastodynamic fundamental solutions for anisotropic solids, *Geophys. J. Int.*, **118**, 384-392 (1994).

[2] C.Y. Wang, Elastic fields produced by a point source in solids of general anisotropy, *Journal of Engineering Mathematics*, **32**, 41-52 (1997).

[3] C.Y. Wang, The stress field of a dislocation loop in an anisotropic solid, *J. Mech. Phys. Solids*, **44**, 293-305 (1996).
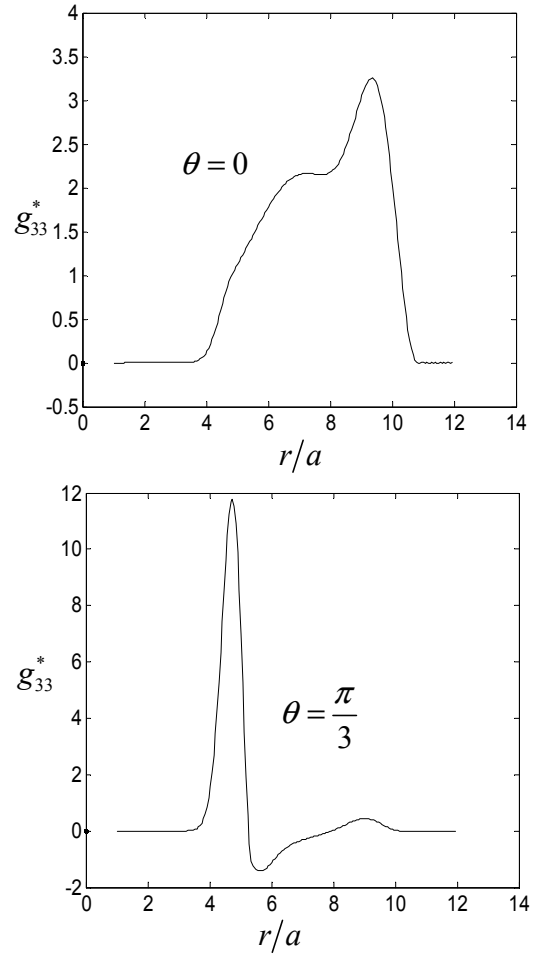

Fig. 10 Dimensionless displacement in ice: $g_{33}^{*} = \left(800\pi^{2}ac_{44} \right) g_{33}\left(x,t \right)$ versus r/a.